Nanoscale Horizons

ROYAL SOCIETY OF CHEMISTRY

COMMUNICATION

View Article Online
View Journal | View Issue



Cite this: *Nanoscale Horiz.*, 2022, 7, 1411

Received 8th July 2022,
Accepted 29th August 2022

DOI: 10.1039/d2nh00322h

rsc.li/nanoscale-horizons



# Bioinspired conductive structural color hydrogels as a robotic knuckle rehabilitation electrical skin†

Wenwen Shao, Lihao Zhang, Zhijun Jiang, Mingtian Xu, Yufei Chen, Sunlong Li and Cihui Liu *

**Electronic skins have attracted significant research interest in the biomedical engineering field including wearable devices, artificial prostheses, software robots, and so on. However, the integration of electronic skin for use in rehabilitation exercise remains unexplored. Here, we propose a novel, conductive structurally colored composite hydrogel for use as a robotic knuckle rehabilitation skin. It was found that the composite structure has an obvious color variation and electromechanical properties during the bending process. Therefore, this film could be used as a multi-signal response electronic skin to achieve real-time color sensing and electrical response, as well as for the human knuckle rehabilitation robot. These results indicated that the structurally colored composite hydrogels are valuable for use in many practical biomedical rehabilitation exercises where they are used as an electronic skin to give real-time color sensing and electrical response, and as well can be used in a human knuckle rehabilitation robot.**

**New concepts**

The novel robotic knuckle rehabilitation electrical skins were constructed with an inverse-opal photonic crystal hydrogel which not only reported the stimuli visually by color change, but also by quantitative feedback stimuli signals from electrical signals. The novel robotic knuckle rehabilitation electrical skins can be controlled by physical bending, NIR radiation and electrical signals which offer people flexible options to exercise. The novel robotic knuckle also showed good rehabilitation application prospects which might be useful for biomedical applications.

## Introduction

As an important part of artificial intelligence, remarkable progress has been made using electronic skin in daily health monitoring, disease diagnosis, in soft robots and so on.[1–3] Nowadays, considerable research work has been devoted to developing new materials or structures with high performance, which are aimed at realizing the perception of dynamic deformation under different physical stimuli.[4,5] Among these materials, a hydrogel is considered as an ideal candidate material for bionic electronic skin due to its excellent flexibility and adjustable mechanical properties.[6] Despite the successes of various functional hydrogels, most hydrogels are derived from synthetic polymers, and their complex extraction or synthesis processes could raise biocompatibility issues.[7] In addition, current strategies for capturing changes in hydrogel-derived electronic skin often require precise and expensive instruments that are relatively bulky, and their use is often limited in outdoor applications that require real-time monitoring.[8–10] Therefore, the production of a conductive film with dual response capability and additional self-report is still expected.

In order to solve these problems, this research used a poly(*N*-isopropylacrylamide-*co*-acrylic acid) [P(NiPAAm-bis-AA)]/poly(ethylene glycol)diacrylate (PEGDA)/reduced graphene oxide (rGO) composite hydrogel film, which had good mechanical properties with ultraviolet (UV) light sensitivity, excellent mechanical properties and brilliant flexibility. Thanks to these advantages, such hydrogels have been widely developed in biomedical fields such as drug delivery, tissue engineering, and electronic skin.[11–13] However, the bioinspired structural colors generated by the interaction of light and periodically ordered structures have attracted much attention in biomedical sensors.[14–16] In particular, when structural colors are combined with soft hydrogels, changes in volume or shape under different stimuli result in visual color changes. This characteristic endows structural color materials with an outstanding self-reporting ability and is of great practical value in sensing visualization, which enables its use in complex applications in biomedical engineering.[17,18] However, the integration of e-skins with structural color for use in rehabilitation exercise remains unexplored.[19]

In this paper, we propose a novel, conductive structural color composite hydrogel for use as robotic knuckle rehabilitation skins, as shown in Fig. 1. The knuckle plays an important

*School of Computer and Electronic Information, Nanjing Normal University, Nanjing, 210000, People's Republic of China. E-mail: cihui@njnu.edu.cn*

† Electronic supplementary information (ESI) available. See DOI: https://doi.org/10.1039/d2nh00322h

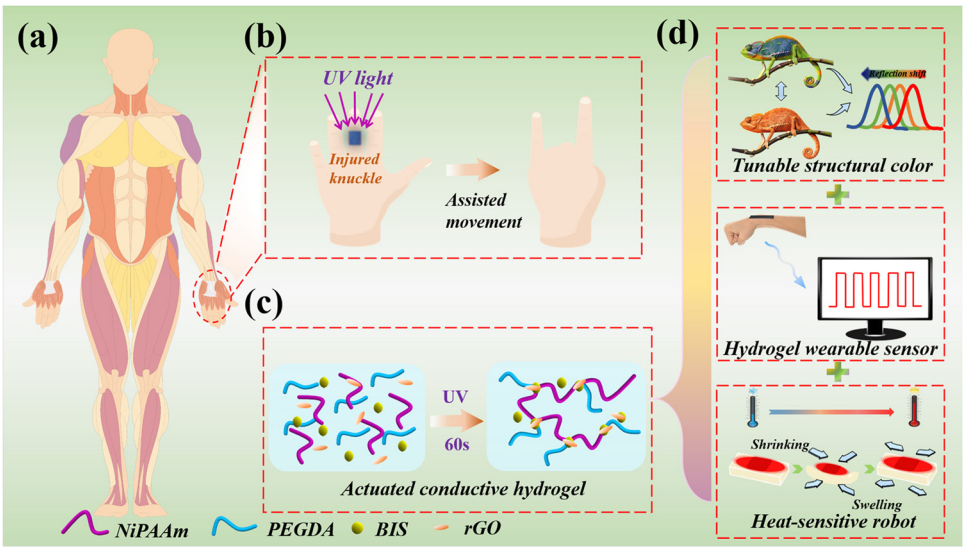


Fig. 1 Stretchable conductive composite hydrogel scheme for knuckle rehabilitation. (a) Schematic of the human body. (b) Further application of a multifunctional hydrogel in a wearable flexible sensor for use in rehabilitation exercises. (c) The composition of the hydrogel and its synthesis method. (d) The multiple properties of composite hydrogels. Inspired by the changeable structural color of a chameleon's body surface, the structural color of the hydrogel film can be adjusted. Wearable hydrogel films contain conductive reduced graphene oxide, which can sense and monitor human motion information in real time. The film is also heat sensitive, which can shrink and swell with the increase and decrease of temperature.

role in the process of human movement, more and more people inadvertently suffer from knuckle disorders during exercise (Fig. 1a). Under UV light, the shrinkage of the hole leads to the shrinkage of the film, so as to assist the rehabilitation of human knuckles (Fig. 1b). The prepared structural color composite hydrogel film, can be used as a wearable electronic sensor to monitor human knuckle movement. Therefore, P(NiPAAm-bis-AA), PEGDA, and rGO were mixed to obtain an inverse-opal membrane (Fig. 1c). While maintaining the original extensibility and flexibility, the hydrogel has excellent mechanical properties, a bright structural color, and high conductivity (Fig. 1d). Inspired by chameleons, it was demonstrated that the composite structure has obvious color variation and electromechanical properties during the bending or extending process.[20–23] Therefore, this film is used as a multi-signal response electronic skin to achieve real-time color variation and electrical responsiveness, as well as for the human knuckle rehabilitation robot.[24–26] These results indicated that the structural colored composite hydrogels are valuable for use in practical biomedical rehabilitation exercises.

## Results and discussion

In a typical experiment, the graphene hybrid structural color hydrogels were first constructed based on the inverse-opal structured hydrogel film using the template sacrifice method. To obtain a colloidal crystal template, the monodispersed silica nanoparticles were self-assembled on the surface of a glass slide and formed a closely packed array by gradually evaporating the solvent. The result was the formation of a close-packed array with a hexagonal arrangement structure, as shown in the scanning electron microscopy (SEM) images (Fig. 2a). The precursor solution of rGO/P(NiPAAm-bis-AA) was prepared and stored in a cold and dark place. Generally, a pre-gel solution was prepared and then injected into the templates. Because of capillary action, the solution infiltrated into the interconnected nanopores between the neighboring nanoparticles and was subsequently polymerized by UV light to form a solidified composite hydrogel. By further etching the silica templates, a free-standing hydrogel film with an inverse-opal scaffold structure appeared, with a periodic porous structure (Fig. 2b).

Inverse-opal hydrogel films have special optical properties, namely a photonic band gap (PBG), due to the periodic arrangement of the internal microstructure. When the material was hit by incident light, the propagation of light was interfered with by these nanopores, and only light of certain wavelengths can be reflected. In general, when the wavelength of light is in the visible range, the inverse-opal structure of the hydrogel film will produce a bright structural color. For the normal incident beam, the position of the reflection peak can be determined by Bragg's formula: $\lambda = 1.633 d n_{\text{average}}$, where $\lambda$ is the wavelength of the reflection peak, $d$ is the center-to-center distance between adjacent nanoparticles, and $n_{\text{average}}$ is the average refractive index of the material. When the center distance between adjacent nanoparticles was constant, the position of reflection peak $\lambda$ is related to $n_{\text{average}}$. Therefore, when the temperature-sensitive P(NiPAAm-bis-AA) was affected by the temperature and the refractive index of the surrounding environment, the inverse-opal photonic crystals showed different reflection peaks and the corresponding bright structural colors (Fig. 2c and Movie S1, ESI†). In addition, the inverse-opal structured hydrogel also gained conductivity after the addition of a conductive

 

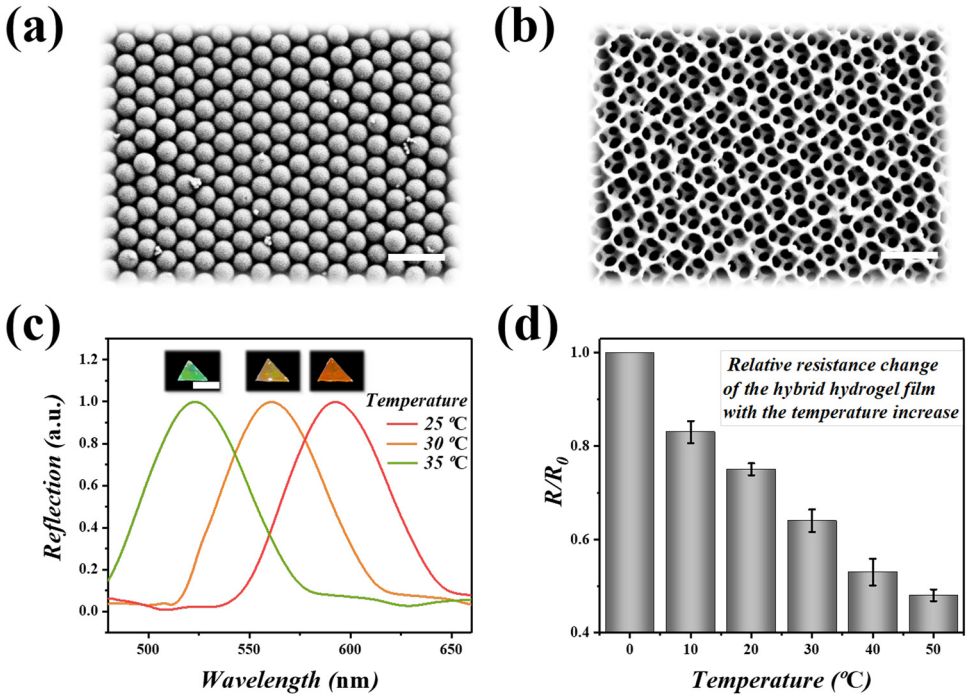


Fig. 2 Characterization of graphene hybrid structural color hydrogels. (a) The SEM image of the colloidal crystal template. (b) The SEM image of the inverse-opal structured hydrogel film. Scale bars in (a and b) are 500 nm. (c) Inverse-opal images and the relationship between the reflectance wavelength and the temperature. Scale bar in (c) is 1 cm. (d) Relative resistance changes with the increase of temperature.

reducing rGO hydrogel filler (Fig. 2d). Increasing the temperature of the hydrogel lead to the shrinkage of the hydrogel film, which lead to the aggregation of the rGO. Therefore, the gap between the rGO decreased and the relative resistance was negatively correlated with the increase of temperature, indicating that the rGO had a good conductivity response to temperature.

To further broaden their practical value, dual-layer hybrid structural color hydrogel films with complex patterns were produced which easily reflected the health of the skin surface (Fig. 3). Based on template molding methods, different patterns including chameleon and crab, were replicated by adding rGO filler to the P(NiPAAm-bis-AA) inverse-opal hydrogel films, could be prepared using a glass slide as the substrate (Fig. 3a). As expected, when the pattern and base were doped with P(NiPAAm-bis-AA), the structure color of the upper and lower layers changed with temperature, as the temperature increased. As is shown in the Fig. 3b, the entire membrane of the pattern changed from red to green when the temperature of the external environment was increased. It was surprising to find that only the pattern at the upper layer changed its structural color, and this was because the base was doped with rGO under electrical stimulation (Fig. 3c). As the image shows, the top layer changed from red to green and then to blue, whereas the base remained green throughout. Next, in order to explore the relationship between the length of the hybrid hydrogel film and the wavelength under different temperatures, a number of tests were carried out (Fig. 3d). In the continuous experiments, it was found that as the temperature of the film increased, its length gradually changed from 3 cm to 2 cm, and its reflection wavelength changed from more than 600 nm to more than 400 nm. In the process, the NIR response rate of the complex patterned hybrid hydrogel film was positively correlated with the irradiation power, as well as the rGO concentration (Fig. 3e). After considering the suitable and controllable condition, the hybrid hydrogel film with the irradiation power of 2.0 A $cm^{-2}$ and an rGO concentration of 4 mg $mL^{-1}$ was used for the subsequent experiments. It could be inferred that the NIR response rate of hybrid hydrogel membrane was positively correlated with the concentration of rGO. The higher the concentration of rGO, the faster the hybrid film increases with temperature. In addition to the visual signals, the relative resistance changes of the hybrid hydrogel films at different concentrations of rGO were also recorded (Fig. 3f). A significant change in relative resistance of the film was observed when the concentration of rGO increased and it dropped to 0.2 when the concentration of rGO was 5 mg $mL^{-1}$, which indicated a good responsiveness to the high concentration stimulation.

As shown previously, the visual dual signal composite hydrogel structure color film showed a great practical value for wearable strain sensors and was used to monitor human knuckle movement and promote knuckle rehabilitation (Fig. 4a). Here, the stimulated knuckle motion was monitored by pasting the designed film directly onto people's fingers. A hose was used instead of a human joint for the stimulation experiment (Fig. 4b). This test was designed to stimulate the membranes' deformation, and to detect the stability of the

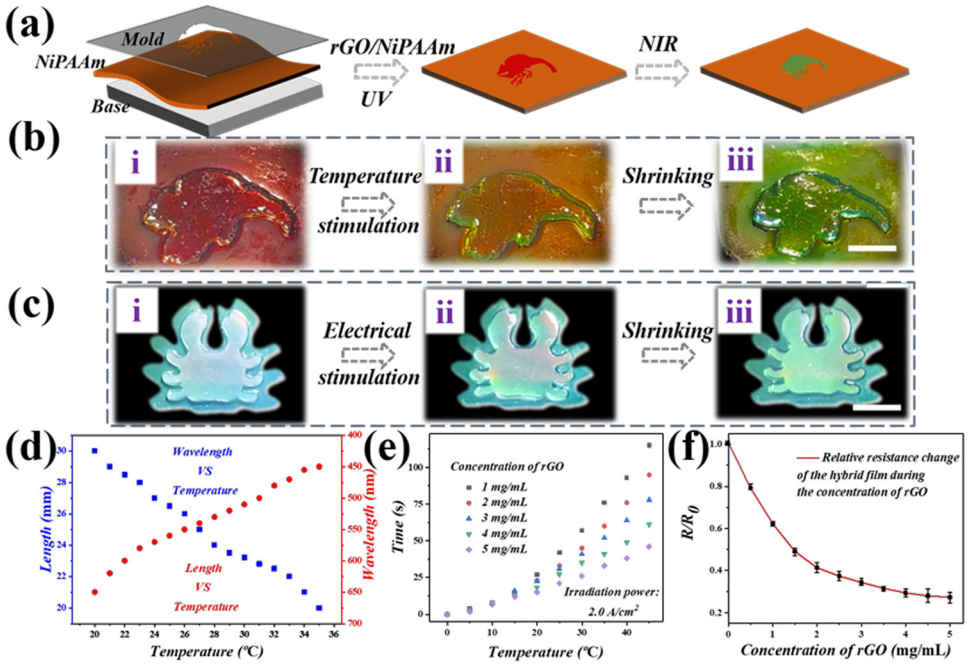


Fig. 3 Temperature response, color-sensing and photo-controllable performance of the hybrid hydrogel films. (a) Schematic illustration of the production of hybrid hydrogel films. (b) Photographs of the chameleon-shaped hybrid hydrogel films with an increase of temperature. (c) Photographs of the crab-shaped hybrid hydrogel films under electrical stimulation. (d) The relationship between the length of the hybrid hydrogel film and wavelength under different temperatures. (e) The relationship between the hybrid hydrogel film temperature and the NIR irradiation time under different rGO concentrations. (f) Relationship between the different rGO concentrations and relative resistance of the hybrid hydrogel films. The scale bar in (b and c) is 1 cm.

films (Movies S2 and S3, ESI†). When the hydrogel film attached to the rubber tube was bent, the structural color changed significantly. The structure color turned bluer as the degree of bending became larger, whereas the part that was not bent remained green. This phenomenon showed that the bending of the film could be visualized by changes in the structural color, which also reflected the degree of bending. In Fig. 4c, a film with bright structural color was stuck onto the knuckles, and then the fingers were then used to lift dumbbells. The films show different structural colors, and their

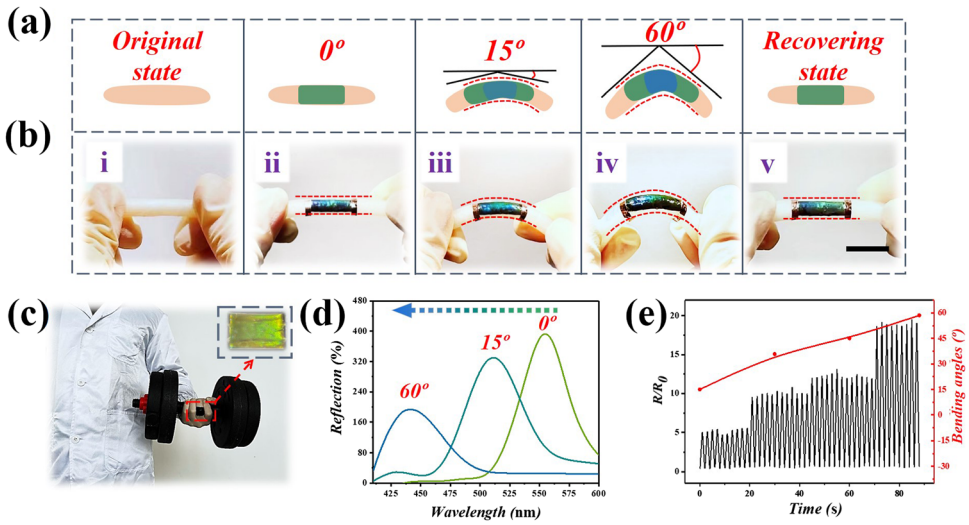


Fig. 4 The changes of optical and electrical signals of the composite hydrogel film during the bending process. (a) Schematic illustration of the hybrid hydrogel films. (b) A stimulation experiment with a hose. Optical images of the hydrogel films attached to the rubber tube being bent at different angles, and the state of the membranes after the removal of external forces. The scale bar is 1 cm. (c) Dumbbell exercises are performed by attaching a hydrogel film to a human knuckle. (d) The reflection peak wavelengths of composite hydrogel films at different bending angles. (e) The relative resistance variation of the composite hydrogel film under cyclic changes of different angles. Scale bar is 1 cm.

 

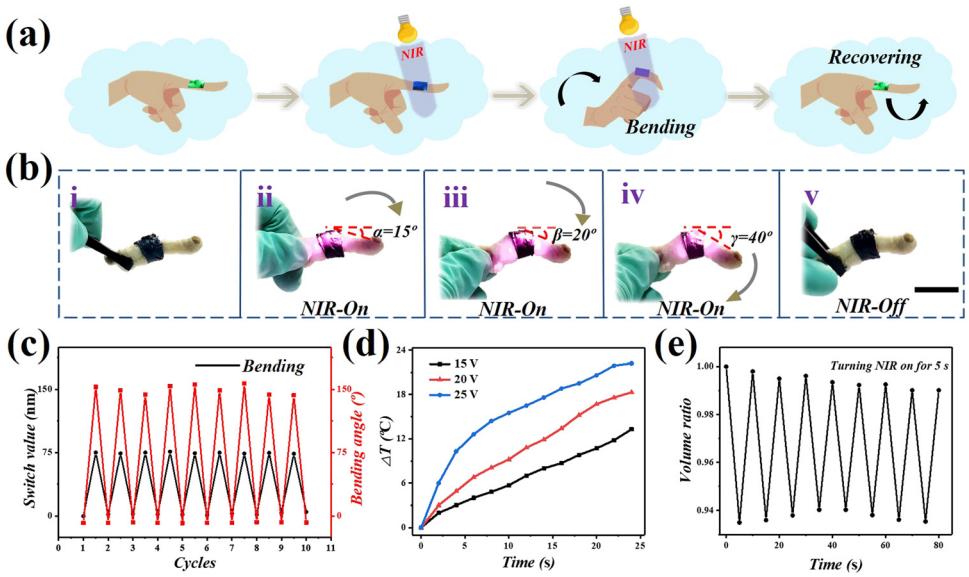


Fig. 5 (a) A schematic diagram of a thin-coated finger illuminated with infrared light. (b) A stimulation experiment was conducted with a chicken claw. Optical images of the hydrogel films attached to the toes of the chicken feet being illuminated by infrared light, and the state of the membranes after the removal of infrared light. (c) The switch value of the reflection peak as well as the bending angle of the hydrogel film as a function of the heating cycle numbers. (d) The relationship between the temperature of the hybrid hydrogel film with input voltage and input time. (e) The real-time volume ratio changes of the hybrid hydrogel film with NIR light switched on for 5 s. Scale bars are 1 cm.

spectrograms are shown in Fig. 4d. At the same time, the change of relative resistance during finger bending was recorded in real time. It is worth noting that when the knuckles were repeatedly bent at the same angle, the resistance changes of the membrane remained stable, indicating that the composite hydrogel membrane had a stable and sensitive electrical conductivity during dynamic activity (Fig. 4e). Therefore, the composite hydrogel structural film not only had a wide source of polymer materials, but also had excellent mechanical properties, electrical conductivity, and a unique dual signal reporting capability, as an electronic skin, with a great potential for use in future applications.

Because of these outstanding features, the hybrid hydrogel films show good prospects for use in wearable electronics (Fig. 5a). In order to explore its potential, a hybrid hydrogel film was fabricated and attached to the fingers of chicken feet. A stimulation experiment with a chicken claw, was conducted as shown in Fig. 5b and Fig. S2 (ESI†). Under the NIR, the joint where the film was attached began to bend. As can be seen in the image, the chicken claw joint changed from 15° to 40° under the stimulation of NIR. Surprisingly, the film returned to its original state after the infrared light was removed. In order to figure out the relationship between films' bending angle and structural color, we stuck the film on the chicken paw joint and bent it repeatedly. The switch value of the reflection peak, as well as the bending angle of the hydrogel film changed with the heating cycle numbers (Fig. 5c). It could be seen that the film with structural color showed rapid changes, and had a durable cycle test performance, according to the deformations caused by knuckle bending (Fig. S4, ESI†). In the process, because of the small resistance of rGO, the input of voltage could be transformed into heat, warming up the hybrid hydrogel film and inducing the shrinkage of the rGO/P(NiPAAm-bis-AA) layer, which further led to the structural color variation of the hybrid hydrogel film. With the increase of voltage and working time, the temperature of the hybrid hydrogel film was gradually elevated (Fig. 5d). Furthermore, real-time volume ratio changes of the hydrogel films were recorded under 5 s of NIR irradiation (Fig. 5e).

## Conclusion

A color film with a double-response conductive structure was developed by adding conductive rGO/P(NiPAAm-bis-AA) filler into an inverse-opal structure scaffold. The results show that due to the adjustable temperature response of the P(NiPAAm-bis-AA) polymer, the volume or internal nanostructure of the film can be changed under the stimulation of temperature, and the inverse-opal scaffold gives the film a bright structural color. In addition, due to the addition of the rGO, the hybrid film showed excellent conductivity. More importantly, because of the extraordinary NIR photothermal conversion ability of the rGO, this hybrid film with a temperature-sensitive polymer component can be endowed with photo-response characteristics. In addition, the hybrid film can not only feedback electrical signals, but can also visually display color changes in response to temperature stimuli. In addition, the hybrid membrane shows great potential in the rehabilitation of human knuckles. Therefore, the structure color film with a hybrid conductive structure has broad application prospects in the field of flexible electronics.

# Experimental section

### Materials

The monomers used to prepare the hydrogel were acrylic acid (AA, Sigma-Aldrich) and *N*-isopropylacrylamide (NiPAAm, Sigma-Aldrich). *N*,*N*′-methylene bisacrylamide (BIS, Sigma-Aldrich) and 2-hydroxy-2-methyl-1-phenyl-propanone (HMPP) were used as a crosslinking agent and a thermal initiator, respectively. Hydrofluoric acid (HF) was obtained from the Aladdin Industrial Corporation. The rGO aqueous solutions were purchased from Nanjing XFNANO Materials Tech. The surfactant added to the rGO aqueous solution was poly(vinylpyrrolidone). The water used in all the experiments was purified using a Milli-Q Plus 185 water purification system (Millipore, Bedford, MA, USA) with a resistivity higher than 18 MΩ cm.

### Preparation of silica nanoparticles

Anhydrous ethanol, ammonia and deionized water were placed in a 500 mL three-necked flask equipped with a stirrer and a thermometer. The mixture was stirred in a constant temperature water bath (37 °C) for 1 h. Then, tetraethyl orthosilicate (TEOS) was added dropwise with continuous stirring. By controlling the amount of TEOS used and the reaction time, the $SiO_2$ nanoparticle solutions with diameters of 265 nm and 290 nm were obtained. Next, the synthesized solution was centrifuged and the precipitate was washed with ethanol and deionized water. Finally, the $SiO_2$ nanoparticles were acquired after drying in an oven.

### Preparation of the P(NiPAAm-bis-AA) inverse-opal film

The P(NiPAAm-bis-AA) inverse opal film was prepared using a sacrificial template method. The P(NiPAAm-bis-AA) hydrogel solution with a concentration of about 10% was prepared from NiPAAAm (9.72 mmol) and BIS (0.81 mmol) in a ratio of 29 : 1, with addition of deionized water (34.7 mmol). The rGO aqueous solution (1, 2, 3, 4, or 5 mg $mL^{-1}$) was added to the mixture at a concentration of 2 mg $mL^{-1}$. Then the P(NiPAAm-bis-AA) hydrogel solution was injected into the gap of a silica colloidal crystal film, and was then irradiated with UV light, through the mask, for 100 s before curing. The hydrogel outside the membrane was removed mechanically. Then, the cured hydrogel was corroded using HF to obtain the required hydrogel film.

### Preparation of dual-responsive graphene hybrid structural color hydrogels

A layer of the conductive P(NiPAAm-bis-AA) was used a base for the preparation of the hybrid structure color hydrogel. Firstly, the pre-gel solution of rGO/P(NiPAAm-bis-AA) was prepared. The monomer P(NiPAAm-bis-AA) and the crosslinked BIS were mixed in a weight ratio of 29 : 1, and the final concentration of the solution was 30 wt%. Next, the photo initiator, HMPP (1%, v/v) was added to the mixture. Different concentrations of rGO (1, 2, 3, 4, 5 mg $mL^{-1}$) were added to the pre-gelatinized solution of rGO-P(NiPAAm-bis-AA) and ultrasonic treatment was performed at room temperature until a uniform solution was obtained. Next, the rGO/P(NiPAAm-bis-AA) solution was injected into the voids of the three-dimensional photonic crystal film. The hybrid hydrogel was irradiated by UV light at 0 °C, and a double-response graphene hybrid structure color film was obtained. The typical thickness of the mixed color film was 1 mm. During heating/radiation, the thickness of the film remained constant. In addition, the color of the hybrid structure color film depended on the viewing angle, and the reflection peak of the hybrid structure color film was recorded from a fixed vertical observation position. The color of the hybrid color film was insensitive to humidity change. The mixed structure color film was dried and stored in a sealed and stable environment, but it still allowed it to absorb moisture during application.

### Construction of a patterned double-response graphene hybrid color hydrogel

Chameleon and crab-shaped hybrid structure color hydrogels were prepared by injecting P(NiPAAm-bis-AA) pre-gel solution into a silica template and it was exposed to UV light under a chameleon or a crab pattern mask mold. Then, the rGO/P(NiPAAm-bis-AA) solution was immersed in the chameleon or crab-shaped P(NiPAAm-bis-AA) inverse-opal scaffold membrane. Finally, it was polymerized irradiation with UV light at 0 °C to obtain the colored hydrogel with a chameleon or crab-shaped hybrid structure. With P(NiPAAm-bis-AA) inverse-opal scaffold film as the substrate, the rGO/P(NiPAAm-bis-AA) solution was injected into the gap of the P(NiPAAm-bis-AA) inverse opal scaffold films. The mask mold either chameleon or crab-shape was placed on the rGO/P(NiPAAm-bis-AA) solution, and the solution was polymerized at 0 °C using UV light. By removing the unpolymerized solution, the colored hydrogel with the desired shape was obtained. During the heating/radiation process, the electric heating thermostat NIR as a light source lead to uneven heating and uneven color change of patterned mixed structure color hydrogel.

# Author contributions

C. H. L., W. W. S., Z. X. G., and Y. S. D. conceived the idea and designed the experiment. X. R. Z. and C. H. L. conducted the experiments and wrote the paper. X. R. Z., W. W. S., and C. H. L. analyzed the data. All the authors contributed to the preparation of the manuscript.

# Data and materials availability

All data needed to evaluate the conclusions in the paper are present in the paper and/or the ESI.† Additional data related to this paper may be requested from the authors.

# Conflicts of interest

The authors declare that they have no competing interests.

 

## Acknowledgements

This work was supported by the National Natural Science Foundation of China (Grant No: 21802074), and by funding from the Nanjing Normal University.

## References

1 J. Xu, H. C. Wu, C. Zhu, A. Ehrlich, L. Shaw, M. Nikolka, S. Wang, F. Molina-Lopez, X. Gu, S. Luo, D. Zhou, Y. H. Kim, G. N. Wang, K. Gu, V. R. Feig, S. Chen, Y. Kim, T. Katsumata, Y. Q. Zheng, H. Yan, J. W. Chung, J. Lopez, B. Murmann and Z. Bao, *Nat. Mater.*, 2019, **18**, 594–601.
2 Z. Lei, W. Zhu, X. Zhang, X. Wang and P. Wu, *Adv. Funct. Mater.*, 2020, **31**, 2008020.
3 X. Yu, Z. Xie, Y. Yu, J. Lee, A. Vazquez-Guardado, H. Luan, J. Ruban, X. Ning, A. Akhtar, D. Li, B. Ji, Y. Liu, R. Sun, J. Cao, Q. Huo, Y. Zhong, C. Lee, S. Kim, P. Gutruf, C. Zhang, Y. Xue, Q. Guo, A. Chempakasseril, P. Tian, W. Lu, J. Jeong, Y. Yu, J. Cornman, C. Tan, B. Kim, K. Lee, X. Feng, Y. Huang and J. A. Rogers, *Nature*, 2019, **575**, 473–479.
4 J. Guo, Y. Yu, D. Zhang, H. Zhang and Y. Zhao, *Research*, 2021, **2021**, 7065907.
5 J. Ma and C. Wu, *Exploration*, 2022, **2**, 20210083.
6 B. B. Gao, X. Wang, T. Li, Z. Q. Feng, C. Y. Wang and Z. Z. Gu, *Adv. Mater. Technol.*, 2019, **4**, 1800392.
7 X. Zhang, G. Chen, Y. Yu, L. Sun and Y. Zhao, *Research*, 2020, **2020**, 3672120.
8 Z. Zhang, Z. Chen, Y. Wang and Y. Zhao, *Proc. Natl. Acad. Sci. U. S. A.*, 2020, **2020**, 3672120.
9 T. Y. Xue, H. G. Yang, B. Shen, F. Y. Li, M. Su, X. T. Hu, W. T. Liu and Y. L. Song, *J. Mater. Chem. C*, 2019, **7**, 6317–6322.
10 B. Dai, K. Li, L. X. Shi, X. Z. Wan, X. Liu, F. L. Zhang, L. Jiang and S. T. Wang, *Adv. Mater.*, 2019, **31**, e1904113.
11 H. Liu and S. Wang, *Sci. China: Chem.*, 2014, **57**, 552–557.
12 P. Zhang, H. Chen, L. Li, H. Liu, G. Liu, L. Zhang, D. Zhang and L. Jiang, *ACS Appl. Mater. Interfaces*, 2017, **9**, 5645–5652.
13 R. X. Wang, M. C. Wang, C. Wang, Q. L. Yang, J. M. Wang and L. Jiang, *ACS Appl. Mater. Interfaces*, 2019, **11**, 37365–37370.
14 X. Zhang, C. Liu, L. Zhang, L. Jia, M. Shi, L. Chen, Y. Di and Z. Gan, *Adv. Funct. Mater.*, 2021, 2010406.
15 L. Zhang, L. Sun, Z. Zhang, Y. Wang, Z. Yang, C. Liu, Z. Li and Y. Zhao, *Chem. Eng. J.*, 2020, **394**, 125008.
16 C. Liu, L. Zhang, X. Zhang, Y. Jia, Y. Di and Z. Gan, *ACS Appl. Mater. Interfaces*, 2020, **12**, 40979–40984.
17 J. Kim, M. Lee, H. J. Shim, R. Ghaffari, H. R. Cho, D. Son, Y. H. Jung, M. Soh, C. Choi, S. Jung, K. Chu, D. Jeon, S.-T. Lee, J. H. Kim, S. H. Choi, T. Hyeon and D.-H. Kim, *Nat. Commun.*, 2014, **5**, 5754.
18 J. N. Wang, Y. Q. Liu, Y. L. Zhang, J. Feng, H. Wang, Y. H. Yu and H. B. Sun, *Adv. Funct. Mater.*, 2018, **28**, 1800625.
19 H. Luo and B. Gao, *Eng. Regener.*, 2021, **2**, 163–170.
20 Y. Huang, L. Liu, X. Yang, X. Zhang, B. Yan, L. Wu, P. Feng, X. Lou, F. Xia, Y. Song and F. Li, *Small*, 2021, **17**, e2006723.
21 Z. Ma, J. Ai, Y. Shi, K. Wang and B. Su, *Adv. Mater.*, 2020, **32**, e2006839.
22 Y. Chen, B. Dang, J. Fu, J. Zhang, H. Liang, Q. Sun, T. Zhai and H. Li, *ACS Nano*, 2022, **16**, 7525–7534.
23 H. Liu, H. Wang, H. Wang, J. Deng, Q. Ruan, W. Zhang, O. A. M. Abdelraouf, N. S. S. Ang, Z. Dong, J. K. W. Yang and H. Liu, *ACS Nano*, 2022, **16**, 8244–8252.
24 X. Wu, J. Zhu, J. W. Evans and A. C. Arias, *Adv. Mater.*, 2020, **32**, e2005970.
25 Y. Zhao, L. Song, Z. Zhang and L. Qu, *Energy Environ. Sci.*, 2013, **6**, 3520–3536.
26 Z. Zhang, Z. Chen, L. Sun, X. Zhang and Y. Zhao, *Nano Res.*, 2019, **12**, 1579–1584.